Full Paper

Multilayer Assembly of Hemoglobin and Colloidal Gold Nanoparticles on Multiwall Carbon Nanotubes/Chitosan Composite for Detecting Hydrogen Peroxide

Shihong Chen, Ruo Yuan, Yaqin Chai, Bing Yin, Yang Xu*

College of Chemistry and Chemical Engineering, Key Laboratory on Luminescence and Real-Time Analysis, Ministry of Education, Southwest University, Chongqing 400715, P. R. China
*e-mail: yuanruo@swu.edu.cn

Received: April 25, 2008
Accepted: July 10, 2008

Abstract
Chitosan (CS) was chosen for dispersing multi-wall carbon nanotubes (MWNTs) to form a stable CS-MWNTs composite, which was first coated on the surface of a glassy carbon electrode to provide a containing amino groups interface for assembling colloidal gold nanoparticles (GNPs), followed by the adsorption of hemoglobin (Hb). Repeating the assembly step of GNPs and Hb resulted in $\{Hb/GNPs\}_n$ multilayers. The assembly of GNPs onto CS-MWNTs composites was confirmed by transmission electron microscopy. The consecutive growth of $\{Hb/GNPs\}_n$ multilayers was confirmed by cyclic voltammetry and UV-vis absorption spectroscopy. The resulting system brings a new platform for electrochemical devices by using the synergistic action of the electrocatalytic activity of GNPs and MWNTs. The resulting biosensor displays an excellent electrocatalytic activity and rapid response for hydrogen peroxide. The linear range for the determination of H_2O_2 was from 5.0×10^{-7} to 2.0×10^{-3} M with a detection limit of 2.1×10^{-7} M at 3σ and a Michaelis–Menten constant K_M^{app} value of 0.19 mM.

Keywords: Carbon nanotubes, Colloidal gold nanoparticles, Hemoglobin, Layer-by-layer assembly, Hydrogen peroxide, Biosensors

DOI: 10.1002/elan.200804303

1. Introduction

Carbon nanotubes (CNTs) have been extensively studied for their properties and possible application since their discovery in 1991 by Iijima [1]. They exist as two fundamental forms, singlewall and multiwall CNTs. It has been demonstrated that CNTs not only show excellent electrocatalytic activity toward many important biomolecules such as dopamine, NADH and ascorbic acid [2–4] but also have an ability to achieve the direct electron transfer of redox proteins [5–9]. These properties make them extremely attractive for constructing electrochemical sensing devices. However, a key barrier for developing CNTs-based biosensing devices is the insolubility of CNTs in most solvents. Dispersion agents used for the dispersion of CNTs include acetone, dimethylformamide, Nafion, chitosan (CS) and surfactants such as poly(styrene sulfonic acid) sodium (PSS), sodium dodecyl sulfate (SDS) and diallyldimethylammonium chloride (PDDA), and so on. Among these dispersants, CS fulfils many of requirements for preparing a robust, electrochemically active film composed of CNTs [10]. Furthermore, CS is a natural cationic polymer with abundant amino groups. Due to its good biocompatibility, nontoxicity and excellent film forming ability, it has been widely used as an immobilization matrix for biomolecules. Biosensors based on the CS-CNTs composite have been widely reported [10–13].

Just recently, nanocomposites composed of CNTs and transition metallic nanoparticles including gold (Au), platinum (Pt), palladium (Pd), copper (Cu) and silver (Ag), have gained a growing interest. With improved electrocatalytic activity of individual components due to the synergistic effect, they have been widely used for the construction of electrochemical sensing devices. For example, Hrapovic et al. [14] developed a sensitive glucose biosensor based on a composite of platinum nanoparticles and CNTs. Yang et al. [15] fabricated layer-by-layer self-assembled multilayer films of CNTs and platinum nanoparticles with polyelectrolyte (PSS). Due to high sensitivity and fast response of this multilayer film to H_2O_2, a cholesterol biosensor was prepared. Xiang et al. [11] constructed a H_2O_2 biosensor based on the immobilization of cytochrome c on a gold nanoparticles–chitosan–carbon nanotubes nanohybrid film. Additionally, a H_2O_2 biosensor based on a nanohybrid film of gold nanoparticles and CNTs for immobilizing microperoxidase has also been reported [16].

Layer-by-layer (LBL) assembly technique, as a preparative method of organized thin films, has been considered as one of the most promising methods for preparing protein films because of its simple procedure and precise control

over the film composition. By alternate adsorption of charged proteins and oppositely charged polyelectrolytes, LBL construction of protein/polyelectrolytes flims could be achieved [17–19]. Another effective method to construct multilayered protein films is based on the LBL assembly of proteins and nanoparticles. The surface of some nanoparticles could contain positive or negative charges under specific process of synthesis, which facilitates the electrostatic adsorption between nanoparticles and oppositely charged proteins. Furthermore, nanoparticles possess some virtues such as large surface area, good biocompatibility and suitability for surface immobilization mechanism. Lvov and co-worker [20] obtained multilayer Mb films through LBL assembly with MnO_2 or SiO_2. Kunitake and co-workers [21] fabricated LBL films of cytochrome c and TiO_2 nanoparticles on mercaptoethanol modified Au substrates. Patosky et al. [22] achieved multilayered microperoxidase-11/Au nanoparticle films, which exhibited an electrocatalytic activity for the reduction of H_2O_2.

In the present work, CS was chosen for dispersing MWNTs to form stable CS-MWNTs composites, which could easily attach colloidal gold nanoparticles (GNPs) to achieve the nanocomposites of CNTs and GNPs by virtue of the high affinity of amino groups of CS for GNPs [23]. Through LBL assembly of negatively charged GNPs and oppositely charged Hb, $\{Hb/GNPs\}_n$ multilayer films were built on a CS-MWNTs composite film modified electrode. Compared with those systems based on the enzymes immobilized onto the composite of CNTs and other nanomaterials by co-depositing [24], physically entrapping or incorporating [25], and cross-linking using glutaric dialdehyde [15], our presented system based on the LBL assembly of proteins and nanoparticles on the CS-MWNTs composite matrix possesses superior performance with regard to controlled enzyme loading and facile preparation of biosensors. Furthermore, the resulting system, i.e., $\{Hb/GNPs\}_n$/CS-MWNTs film retains well the bioactivity of immobilized Hb. This would ascribe to the fact that both CS and GNPs provide a favorable microenvironment for retaining biological activity of enzymes. Such a modification technology demonstrated in this paper brings a new platform for electrochemical devices by using the synergistic action of the electrocatalytic activity of GNPs and MWNTs.

2. Experimental

2.1. Materials

The multiwall carbon nanotubes (MWNTs) were obtained from Chengdu Organic Chemicals CO. Ltd. Prior to use, MWNTs were refluxed in concentrated nitric acid for about 7 h, then filtered and washed with double-distilled water until the filtrate became neutral, and finally dried under vacuum. Chitosan (CS, Mw: 100 000 – 300 000, deacetylating grade: 70 – 85%), hemoglobin (Hb), gold chloride tetrahydrate and sodium citrate were purchased from Sigma Chemical Co. (St. Louis, MO, USA) and used as received. A stock solution of 1.0 mg/mL Hb was freshly prepared with 0.1 M phosphate buffer solutions (pH 6.0). Hydrogen peroxide (H_2O_2, 30% w/v solution) was purchased from Chemical Reagent Company, Chongqing, China. The diluted H_2O_2 solutions were freshly prepared from this material before amperometric testing and the concentration was determined by titration with potassium permanganate. Furthermore, dissolved O_2 was removed from H_2O_2 by highly pure nitrogen before injecting it into cell. Phosphate buffer solutions (PBS) with various pH values were prepared with 0.1 M KH_2PO_4 and 0.1 M Na_2HPO_4. The supporting electrolyte was 0.1 M KCl. All other chemicals were of analytical grade and used directly without further purification. Doubly distilled water was used throughout the experiments. Colloidal gold nanoparticles with mean size of 16 nm were prepared by reducing gold chloride tetrahydrate with citric acid at 100 °C for half an hour [26].

2.2. Preparation of Modified Electrodes

A 1.0% acetic acid solution was first prepared and then its pH was adjusted to 5.0 using concentrated NaOH solutions. In 10 mL of such acetic acid solution, 50 mg of CS flakes were dissolved by stirring for some time to give a 0.5 wt% CS solution. A CS-MWNTs suspension (1.0 mg/mL) was prepared by dispersing 5 mg of the acid-treated MWNTs into 5 mL of CS solution with the aid of 1 h of ultrasonic agitation.

A glassy carbon (GC) electrode (4 mm in diameter) was first polished with 1.0, 0.3 and 0.05 μm alumina slurry, respectively, and ultrasonically cleaned in ethanol and water and dried in air. Then, 15 μL of CS-MWNTs suspension was cast on a cleaned GC electrode surface. After solvent water was evaporated, the CS-MWNTs/GC electrode was immersed into a colloid gold solution for 8 h to attach GNPs. Subsequently, $\{Hb/GNPs\}_n$ multilayer films were grown on the CS-MWNTs composite film through alternate LBL adsorption from Hb solution (1.0 mg/mL) and colloidal gold solution for 40 min to produce a $\{Hb/GNPs\}_n$/CS-MWNTs/GC electrode. Each immersion was followed by washing with water and drying in a nitrogen stream. The preparation process of the modified electrode is shown in Scheme 1. For comparison, a $\{Hb/GNPs\}_n$/CS/GC electrode without MWNTs and a Hb/CS-MWNTs/GC electrode without GNPs were fabricated. In addition, an electrode only modified with CS-MWNTs was also fabricated. Modified electrodes were stored in a refrigerator (4 °C) until further use.

For UV-vis spectroscopic study, the assembling procedure of $\{Hb/GNPs\}_n$ multilayer films was performed on the clean quartz slides, i.e., the two internal surfaces of a quartz cell. The quartz surfaces were first carefully cleaned with Piranha solution for 15 min, and then ultrasonically cleaned with water and dried in a nitrogen stream. Subsequently, appropriate amount of 0.5 wt% CS solutions were spread evenly on them to obtain CS thin film by vaporizing water.

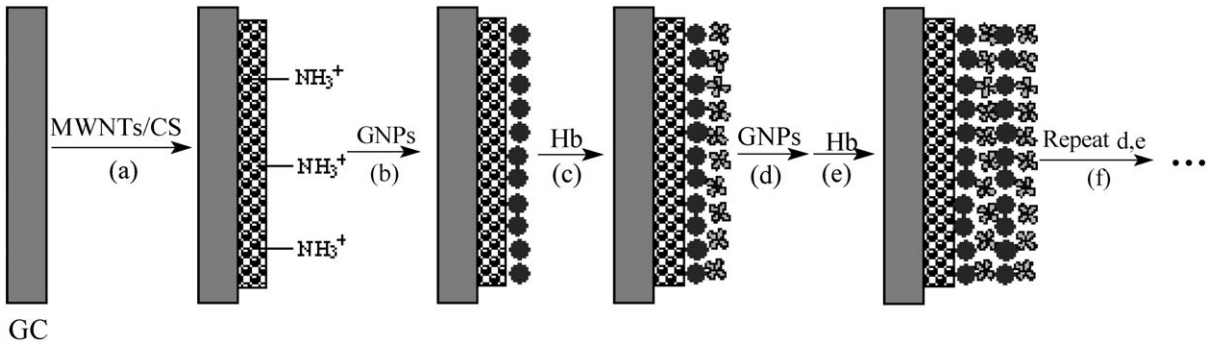

Scheme 1. Illustration of the preparation process of the modified electrode.

Finally, $\{Hb/GNPs\}_n$ multilayers were built on the CS film modified quartz slides by alternate adsorption of GNPs and Hb.

2.3. Apparatus and Measurements

Amperometric and cyclic voltammetric experiments were carried out on a CHI 660A electrochemical work station (Shanghai CH Instruments Co., China). A three-electrode electrochemical cell comprising a modified GC electrode as working electrode, a platinum wire auxiliary electrode, and a saturated calomel electrode (SCE) as reference electrode, was employed. All potentials were measured and reported versus the SCE. The test solutions were deoxygenated by highly pure nitrogen for 10 min before electrochemical experiments and a nitrogen atmosphere was maintained during measurements. All the electrochemical experiments were carried out at room temperature.

Transmission electron microscopy (TEM) was performed with a TECNAI 10 (PHILIPS FEI Co., Holland).

UV-vis absorption spectra was recorded using a type of Lambda 17 UV-VIS 8500 (PE Co,USA) with quartz cell (path length 1 cm) at room temperature.

3. Results and Discussion

3.1. Characterization of the Modified Electrode

3.1.1. Transmission Electron Microscopy

In order to confirm the attachment of GNPs onto CS-MWNTs composites, the transmission electron microscopy (TEM) was performed at a CS-MWNTs composite film and a GNPs/CS-MWNTs composite film, respectively. The results are shown in Figure 1. As could be seen from Figure 1, MWNTs were well dispersed in the CS solution (Fig. 1A). The attachment of GNPs onto CS-MWNTs composites was as expected to be homogeneous and evident (Fig. 1B), confirming the feasibility of proposed strategy for producing the composite material of MWNTs and GNPs using CS as linker based on strong binding interactions between GNPs and amino groups of CS.

3.1.2. Cyclic Voltammetric Characterization

The cyclic voltammetric experiments were conducted to monitor the assembling process of $\{Hb/GNPs\}_n$ multilayer films, where n was the number of {Hb/GNPs} bilayer.

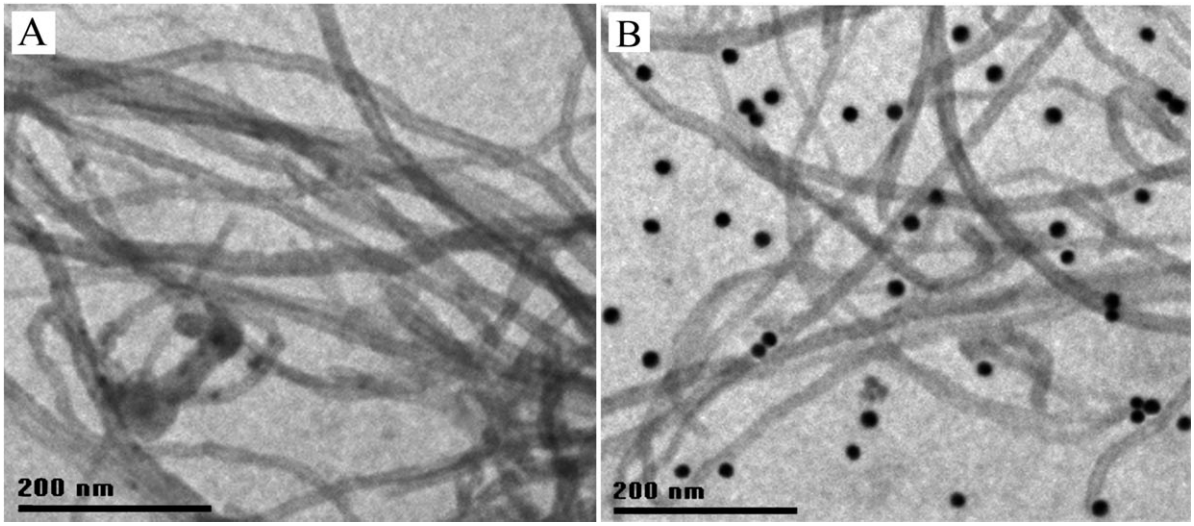

Fig. 1. TEM images of a CS-MWNTs (A) and a GNPs/CS-MWNTs (B) composite film.

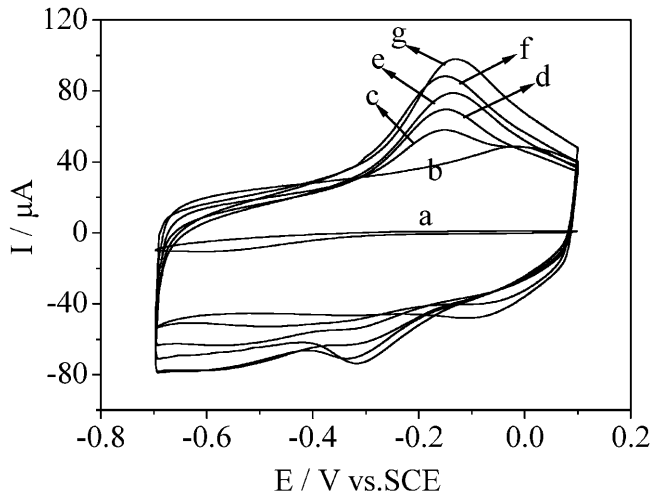

Fig. 2. CVs of different modified electrodes in 0.1 M PBS (pH 6.5) at a scan rate of 50 mV/s: bare GC electrode (a), CS-MWNTs/GC electrode (b), and the electrodes modified with1, 2, 3, 4, 5 layers (from c to g) of {Hb/GNPs} bilayer on the CS-MWNTs film.

Figure 2 displays the cyclic voltammograms (CVs) of different modified electrodes in pH 6.5 PBS at scan rate 50 mV/s. Compared with the bare GC electrode, the background current of CS-MWNTs modified electrode was apparently larger (Fig. 2b), suggesting that an effective electrode surface area was significantly enhanced due to the use of MWNTs. When one bilayer of {Hb/GNPs} was grown on the CS-MWNTs/GC electrode, corresponding CVs displayed a pair of redox peaks (Fig. 2c), while the anodic peak was very obvious and the cathodic peak was not. With the increase of the number of {Hb/GNPs} bilayer, both anodic and cathodic peak currents clearly increased as shown in Figures 2d to 2g and reached a maximum value at the 5 layers. Then a slight decrease of anodic and cathodic peak currents was observed for further increasing the number of {Hb/GNPs} bilayer (here not shown), suggesting the loading of Hb was tended to be saturation at $n=5$. From one to five layers, the increased anodic and cathodic peak currents were attributed to the increase of amount of immobilized Hb on the electrode. In this investigation, we found that the anodic peak was always more obvious than the cathodic peak. Furthermore, the shape of cathodic peak gradually became better with the increase of the number of {Hb/GNPs} bilayer. For $\{Hb/GNPs\}_5$/CS-MWNTs/GC electrode (Fig. 2g), the CVs gave a pair of well-defined redox peaks at -0.13 V and -0.32 V (versus SCE), characteristic of heme Fe(III)/Fe(II) redox couples of Hb, suggesting a quasireversible redox process. So, in our experiment, five layers of {Hb/GNPs} were selected to fabricate a H_2O_2 sensor.

3.1.3. UV-vis Absorption Spectroscopic Characterization

UV-vis absorption spectroscopy was employed to follow the layer-by-layer assembly of $\{Hb/GNPs\}_n$ multilayer films since Hb has a sensitive Soret absorption band at about 412 nm [27] and colloidal gold has a characteristic plasmon absorbance at about 520 nm [28]. Figure 3 displays the UV-vis spectra of colloidal gold solution and $\{Hb/GNPs\}_n$ multilayer films. It can be seen from Figure 3B, the absorbance of Hb at 412 nm and GNPs at 548 nm in $\{Hb/GNPs\}_n$ multilayer films was clearly visible. Compared with the solution spectrum ($\lambda_{max}=518$ nm) of colloidal gold (curve a in Fig. 3A), the absorption bands of GNPs in $\{Hb/GNPs\}_n$ multilayer film had a large red shift and gave a λ_{max} at about 548 nm (curve b in Fig. 3A), this case was similar to those observed for gold nanoparticles modified by PyDDP (*O*,*O*′-dioctadecane dithiophosphate) [29] and for Nafion/Mb/GNPs film [30], which may be ascribed to the interaction between CS and GNPs and the interaction of Hb and GNPs. In addition, the absorbance at 412 nm presented in $\{Hb/GNPs\}_n$ multilayer films was attributed to the Soret band of Hb, suggesting that presence of Hb in the film. Furthermore, the absorbance at 412 nm for Hb and 548 nm for GNPs was increased linearly with increasing the number of {Hb/GNPs} bilayer from one to five layers, as shown in curve a and curve b in the insert of Figure 3B, respectively.

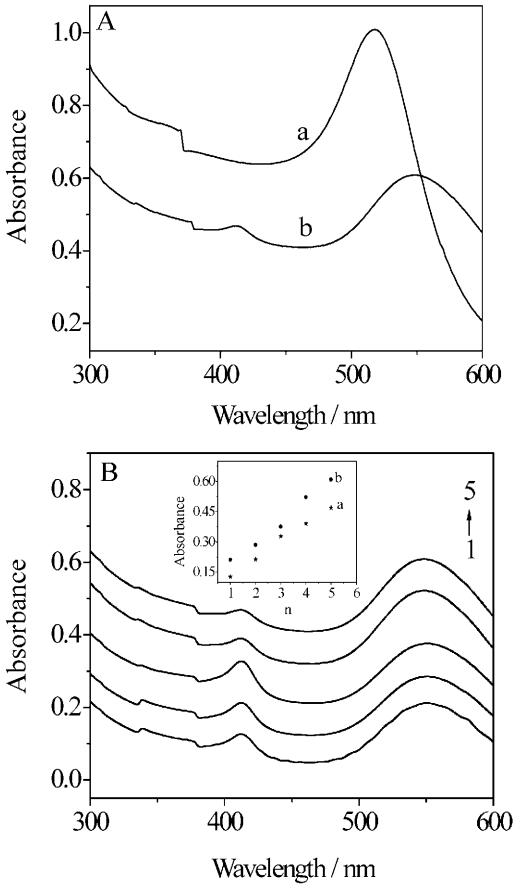

Fig. 3. A) UV-vis absorption spectra of colloidal gold solution (a) and $\{Hb/GNPs\}_5$ films on the CS modified quartz slides (b). B) UV-vis absorption spectra for layer-by-layer $\{Hb/GNPs\}_n$ films on the CS modified quartz slides with different number of bilayers: $n=1-5$. Inset: influence of the number of bilayers (n) on the absorbance at 412 nm (a) and 548 nm (b), respectively.

This confirmed that a $\{Hb/GNPs\}_n$ multilayer film was built up on a CS matrix in a regular and reproducible fashion, and the amount of Hb and GNPs assembled in each bilayer was nearly the same.

3.2. Electrochemical Characteristics of Hydrogen Peroxide Biosensor

The CVs of the $\{Hb/GNPs\}_5$/CS-MWNTs/GC electrode in PBS (pH 6.5) at different scan rates show that both the anodic and cathodic peak currents increase linearly with scan rate from 20 to 300 mV/s, indicating a surface-controlled process.

The electrochemical behavior of the $\{Hb/GNPs\}_5$/CS/MWNTs/GC electrode depends on the pH of the working solution. An increase of pH in solution leads to a negative shift in potential of both cathodic and anodic CV peaks for $\{Hb/GNPs\}_5$/CS/MWNTs/GC electrode (figure not shown). The formal potentials($E^{\circ\prime}$), which is mean of cathodic and anodic peak potentials, have a linear relationship with pH (from 5.0 to 9.0) with the linear equation $E^{\circ\prime}(V) = -0.0482 - 0.0258$ pH, $r = 0.999$). The slope -25.8 mV/pH is obviously smaller than the theoretical value -57.6 mV/pH at 18 °C for a one-proton coupled single-electron transfer during the reversible electrochemical reaction [31]. While the reason for this is not clear yet, the linear correlation between $E^{\circ\prime}$ and pH at least indicates that proton participates in the electron transfer process. The small slope of variation $E^{\circ\prime}$ with pH is also observed in MP-11/GNPs/MWNTs film [16].

The electrocatalytic activity of Hb incorporated in the $\{Hb/GNPs\}_5$/CS-MWNTs film towards hydrogen peroxide was studied by cyclic voltammetry. Figure 4 illustrates the CVs recorded for the $\{Hb/GNPs\}_5$/CS-MWNTs/GC electrode in PBS (pH 6.5) containing varied concentration of H_2O_2 in the absence of oxygen. As can be seen in Figure 4, with the addition of H_2O_2, an obvious increase of reduction peak currents was observed, accompanied by a decrease of oxidation peak currents, indicating a typical electrocatalytic reduction process of H_2O_2.

3.3. Optimum of Analytical Conditions

The analytical conditions including applied potential and pH of test solutions were optimized in order to obtain an efficient biosensor for H_2O_2. The dependence of chronoamperometric current response of the biosensor to constant concentration (8.0×10^{-4} M) H_2O_2 in pH 6.5 PBS on the applied potential in the range from 0 to -550 mV was investigated. The results show that the steady-state current increased rapidly when the applied potential moved from 0 to -400 mV, and approached a plateau at -400 mV (not shown here). Accordingly, a constant potential of -400 mV was selected as the working potential for the determination of H_2O_2. The effect of pH of test solutions on the chronoamperometric current response of the $\{Hb/GNPs\}_5$/CS-MWNTs/GC electrode to constant concentration (8.0×10^{-4} M) H_2O_2 at -400 mV was also investigated (not shown here). The results show that the maximum response appeared at pH 6.5. So the buffer solution of pH 6.5 was employed for the detection of H_2O_2.

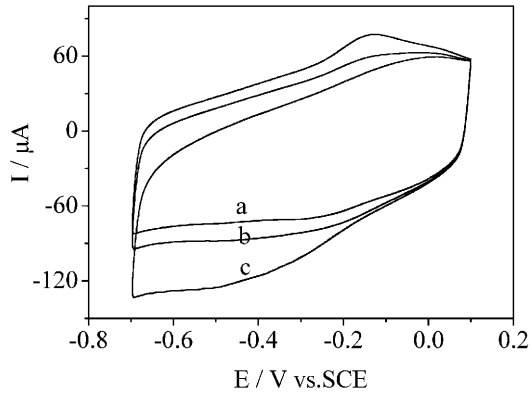

Fig. 4. CVs of the $\{Hb/GNPs\}_5$/CS-MWNTs/GC electrode at a scan rate of 50 mV/s in 0.1 M PBS (pH 6.5) without H_2O_2 (a), with 4.3×10^{-4} (b), and 1.46×10^{-3} (c) M H_2O_2, respectively.

3.4. Amperometric Response of the Biosensor

The amperometric response of the $\{Hb/GNPs\}_5$/CS-MWNTs/GC electrode was investigated by successively adding H_2O_2 to a continuous stirred PBS solution under the optimized conditions. As controlled experiment, the amperometric responses were also measured at the $\{Hb/GNPs\}_5$/CS/GC, CS-MWNTs/GC and Hb/CS-MWNTs/GC electrodes, respectively. The corresponding typical current–time curves are depicted in Figure 5A. As can be observed, the $\{Hb/GNPs\}_5$/CS/GC electrode showed a detectable but very small current response to H_2O_2 (curve a in Fig. 5A). Such a response was mainly ascribed to direct electron transfer (DET) from Hb molecules to the underlying electrodes, which was promoted through the conducting tunnels of GNPs since they could provide the protein molecules more freedom in orientation and reduce the insulating property of the protein shell for DET [32, 33]. At the same time, both CS-MWNTs/GC (curve b) and Hb/CS-MWNTs/GC electrodes (curve c in Fig. 5A) exhibited a relatively small response current to H_2O_2. Whereas, with the addition of H_2O_2, drastic increase in the response current was observed at the $\{Hb/GNPs\}_5$/CS-MWNTs/GC electrode (Fig. 5A curve d). This result demonstrated clearly that the biosensor based on $\{Hb/GNPs\}_5$ multilayer and MWNTs exhibited a better electrocatalytic activity to H_2O_2 due to the synergistic action of MWNTs and GNPs, since they both had an ability to promote the electron transfer between Hb and the underlying electrode. Additionally, for $\{Hb/GNPs\}_5$/CS-MWNTs/GC electrode, the time to achieve 95% of the steady-state current was in less than 8 s, indicating a fast response process.

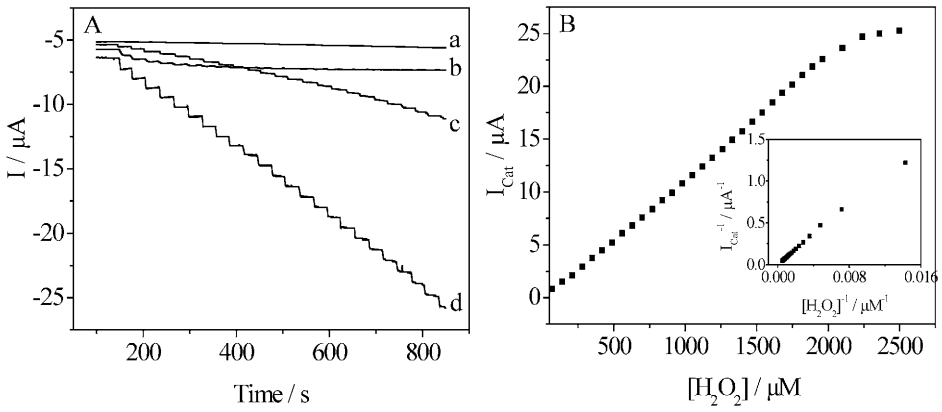

Fig. 5. A) Typical current – time response curves of {Hb/GNPs}$_5$/CS/GC (a), CS-MWNTs/GC (b), Hb/CS-MWNTs/GC (c), and {Hb/GNPs}$_5$/CS-MWNTs/GC (d) electrodes upon successive additions of 70 μM H_2O_2 in pH 6.5 PBS at an applied potential of −400 mV. B) Calibration curve of the {Hb/GNPs}$_5$/CS-MWNTs/GC electrode for H_2O_2 determination. Inset: the Lineweaver – Burk plot.

Figure 5B displays the calibration curve of the {Hb/GNPs}$_5$/CS-MWNTs/GC electrode for H_2O_2 determination under the optimal experimental conditions. The linear response range of the biosensor to H_2O_2 concentration was from 5.0×10^{-7} to 2.0×10^{-3} M with a detection limit of 2.1×10^{-7} M at signal-to-noise ration of three. The linear regression equation of catalytic currents vs. H_2O_2 concentrations was I_{cat} (μA) = −0.3722 + 11.6 [H_2O_2] (mM) with a correlation coefficient of 0.999 (n = 29). Our proposed electrode exhibited a wider response range than the modified electrode based on the immobilization of cytochrome c on a gold nanoparticles – chitosan – carbon nanotubes nanohybrid film [11]. This may be ascribed to the multilayer assembly of Hb. The increase in the quantity of immobilized Hb would result in an increase in response currents.

When the concentration of H_2O_2 was higher than 2.0×10^{-3} M, a response plateau was observed, showing the characteristics of the Michaelis – Menten kinetic mechanism. The apparent Michaelis – Menten constant (K_M^{app}), which gave an indication of the enzyme – substrate kinetics, was calculated to be 0.19 mM according to the Lineweaver – Burk equation [34] (inset in Fig. 5B). This value was smaller than 0.791 mM for Cyt *c*/GNPs/Chit/MWNTs modified electrode [11], 0.857 mM for Cyt *c*/MWNT modified electrode [35], 0.675 mM for Hb-modified CNT powder microelectrodes electrodes [36], 0.32 mM for microperoxidase immobilized on nanohybrid film modified electrode [16]. The low value of K_M^{app} indicated that Hb immobilized in the {Hb/GNPs}$_5$/CS-MWNTs film well retained its bioactivity and had a high biological affinity to H_2O_2.

3.5. Repeatability and Stability of the Hydrogen Peroxide Biosensor

The relative standard deviation (*RSD*) was 3.8 % for nine successive measurements for 0.10 mM H_2O_2 with the proposed biosensor, showing a good reproducibility.

The storage stability of the proposed biosensor was investigated. When not in use, the electrode was suspended above 0.1 M phosphate buffer at 4 °C in a refrigerator. The response to 0.10 mM H_2O_2 was tested intermittently. The results are shown in Figure 6. A gradual loss in the activity of the sensor was observed with the increase of storage period. The response current was maintained at about 81% after storage for one month.

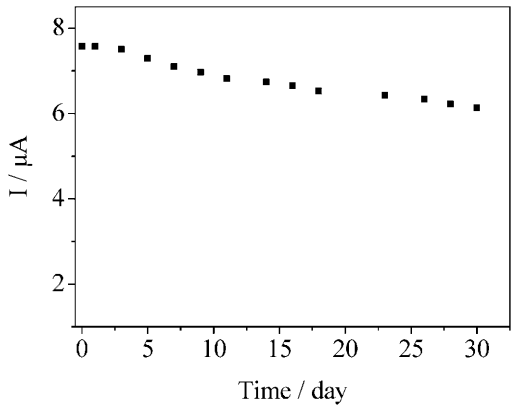

Fig. 6. The storage stability of the proposed biosensor.

3.6. Interference Determination

Five kinds of possible interfering substances, glucose, uric acid, ascorbic acid, L-cysteine and L-tyrosine, were investigated. The degree of interference from interfering substances can be evaluated by comparing the response before and after addition 0.40 mM possible interferents into 0.1 M pH 6.5 PBS containing 0.10 mM H_2O_2. The values of the current ratio, which were calculated by comparing the current of the proposed biosensor in an assay solution containing 0.10 mM H_2O_2 and a 0.40 mM interfering substance with that of the proposed biosensor in the same assay solution containing only 0.10 mM H_2O_2, were 1.02 for glucose, 1.03 for uric acid, 1.06 for ascorbic acid, 0.98 for L-

Table 1. Determination of H_2O_2 in the disinfector sample.

	Determined by biosensor (M) [a]	Determined by potassium permanganate titration method (M) [a]
Disinfector	0.0327 ± 0.0012	0.0366 ± 0.0002

[a] Mean $\pm$ *SD* of three measurements

cysteine and 0.99 for L-tyrosine. It could be concluded that above five tested interferents could not cause observable interference to the determination of H_2O_2, which was largely attributed to the low working potential of -400 mV used in the determination of H_2O_2.

3.7. Real Sample Analysis

The applicability of the proposed biosensor was valuated by detecting H_2O_2 concentration in a disinfector sample. The sample was diluted 20 times with PBS (pH 6.5). H_2O_2 concentration in diluted disinfector sample was tested using the proposed biosensor and the potassium permanganate titration method which was employed as the reference method, respectively. The results are listed in Table 1. It was found that the result obtained by the biosensor was in accordance with that obtained by potassium permanganate titration method, showing the feasibility of using this proposed H_2O_2 biosensor for the H_2O_2 determination in the disinfector sample.

4. Conclusions

In this experiment, a facile strategy for fabricating multilayer films of Hb and GNPs on CS-MWNTs composites was proposed. The resulting system represented a new biocomposite platform for electrochemical devices. Due to the excellent biocompatibility and film forming ability of CS-MWNTs composite, and the synergistic action of GNPs and MWNTs, this proposed system exhibited a highly electrocatalytic activity to H_2O_2. The feasibility of practical application of the proposed biosensor for the H_2O_2 determination has been demonstrated by analyzing the disinfector sample.

5. Acknowledgements

This work was financially supported by the National Natural Science Foundation of China (NO. 20675064), the Natural Science Foundation of Chongqing City (NO. CSTC-2004BB4149, 2005BB4100), and the High Technology Project Foundation of Southwest University (XSGX 02).

6. References

[1] S. Iijima, *Nature* **1991**, *354*, 56.
[2] F. Valentini, A. Amine, S. Orlanducci, M. L. Terranova, G. Palleschi, *Anal. Chem.* **2003**, *75*, 5413.
[3] J. Wang, M. Musameh, *Anal. Chem.* **2003**, *75*, 2075.
[4] S. Chakraborty, C. R. Raj, *J. Electroanal. Chem.* **2007**, *609*, 155.
[5] J. Wang, M. Li, Z. Shi, N. Li, Z. Gu, *Anal. Chem.* **2002**, *74*, 1993.
[6] X. Yu, D. Chattopadhyay, I. Galeska, F. Papadimitrakopoulos, J. F. Rusling, *Electrochem. Commun.* **2003**, *5*, 408.
[7] L. D. Zhu, R. L. Yang, J. L. Zhai, C. Y. Tian, *Biosens. Bioelectron.* **2007**, *23*, 528.
[8] J. J. Gooding, R. Wibowo, J. Q. Liu, W. Yang, D. Losic, S. Orbons, F. J. Mearns, J. G. Shapter, D. B. Hibbert, *J. Am. Chem. Soc.* **2003**, *125*, 9006.
[9] K. Yamamoto, G. Shi, T. S. Zhou, F. Xu, J. M. Xu, T. Kato, J. Y. Jin, L. Jin, *Analyst* **2003**, *128*, 249.
[10] J. Tkac, J. W. Whittaker, T. Ruzgas, *Biosens. Bioelectron.* **2007**, *22*, 1820.
[11] C. L. Xiang, Y. J. Zou, L. X. Sun, F. Xu, *Talanta* **2007**, *74*, 206.
[12] D. Du, X. Huang, J. Cai, A. D. Zhang, *Sens. Actuators B* **2007**, *127*, 531.
[13] M. G. Zhang, W. Gorski, *Anal. Chem.* **2005**, *77*, 3960.
[14] S. Hrapovic, Y. Liu, K. B. Male, J. H. Luong, *Anal. Chem.* **2004**, *76*, 1083.
[15] M. H. Yang, Y. Yang, H. F. Yang, G. L. Shen, R. Q. Yu, *Biomaterials* **2006**, *27*, 246.
[16] Y. Liu, M. K. Wang, F. Zhao, Z. H. Guo, H. J. Chen, S. J. Dong, *J. Electroanal. Chem.* **2005**, *581*, 1.
[17] Y. M. Lvov, Z. Lu, J. B. Schenkman, X. Zu, J. F. Rusling, *J. Am. Chem. Soc.* **1998**, *120*, 4073.
[18] Y. Lvov, K. Ariga, I. Ichinose, T. Kunitake, *J. Am. Chem. Soc.* **1995**, *117*, 6117.
[19] E. J. Calvo, R. Etchenque, L. Pietrasanta, A. Wolosiuk, C. Danilowicz, *Anal. Chem.* **2001**, *73*, 1161.
[20] Y. Lvov, B. Munge, O. Giraldo, I. Ichinose, S. Suib, J. F. Rusling, *Langmuir* **2000**, *16*, 8850.
[21] N. Kimizuka, M. Tanaka, T. Kunitake, *Chem. Lett.* **1999**, *12*, 1333.
[22] F. Patosky, T. Gabriel, I. Willner, *J. Electroanal. Chem.* **1999**, *479*, 69.
[23] J. Li, L. T. Xiao, X. M. Liu, G. M. Zeng, G. H. Huang, G. L. Shen, R. Q. Yu, *Anal. Bioanal. Chem.* **2003**, *376*, 902.
[24] S. H. Lim, J. Wei, J. Y. Lin, Q. T. Li, J. K. You, *Biosens. Bioelectron.* **2005**, *20*, 2341.
[25] M. H Yang, Y. H. Yang, Y. L. Liu, G. L. Shen, R. Q. Yu, *Biosens. Bioelectron.* **2006**, *21*, 1125.
[26] B. V. Enüstün, J. Turkevich, *J. Am. Chem. Soc.* **1963**, *85*, 3317.
[27] J. Yang, N. F. Hu, J. F. Rusling, *J. Electroanal. Chem.* **1999**, *463*, 53.
[28] H. Z. Huang, X. R. Yang, *Colloids Surf. A* **2003**, *226*, 77.
[29] L. Z. Gao, X. T. Zhang, S. X. Dai, Y. C. Li, Y .B. Huang, Z. L. Du, T. J. Li, *Acta Phys. –Chim. Sin.* **2004**, *20*, 647.
[30] W. W. Yang, Y. C. Li, Y. Bai, C. Q. Sun, *Sens. Actuators B* **2006**, *115*, 42.
[31] A. M. Bond, *Modern Polarographic Methods in Analytical Chemistry*, Marcel Dekker, New York **1980**.
[32] J. Zhao, R. W. Henkens, J. Stonchuerner, J. P. O'Daly, A. L. Crumbliss, *J. Electroanal. Chem.* **1992**, *327*, 109.
[33] A. L. Crumbliss, J. G. Stonchuerner, R. W. Henkens, J. Zhao, J. P. O'Daly, *Biosens. Bioelectron.* **1993**, *8*, 331.
[34] R. A. Kamin, G. S. Wilson, *Anal. Chem.* **1980**, *52*, 1198.
[35] G. C. Zhao, Z. Z. Yin, L. Zhang, X. W. Wei, *Electrochem. Commun.* **2005**, *7*, 256.
[36] Y. D. Zhao, Y. H. Bi, W. D. Zhang, Q. M. Luo, *Talanta* **2005**, *65*, 489.

